

Title page

Title: *In vivo* pharmacokinetic and pharmacodynamic properties of the antiarrhythmic molecule *ent*-verticilide

Authors: Daniel J. Blackwell, Abigail N. Smith, Tri Do, Aaron Gochman, Jeffrey Schmeckpeper, Corey R. Hopkins, Wendell S. Akers, Jeffrey N. Johnston, Bjorn C. Knollmann

Affiliations: Department of Medicine, Vanderbilt University Medical Center, Nashville, TN (D.J.B., J.S., B.C.K.); Department of Chemistry and Vanderbilt Institute of Chemical Biology, Vanderbilt University, Nashville, TN (A.N.S., J.N.J.); Department of Pharmacology, Vanderbilt University, Nashville, TN (A.G., W.S.A.); Pharmaceutical Sciences Research Center, Lipscomb University, Nashville, TN (T.D., W.S.A.); Department of Pharmaceutical Sciences, College of Pharmacy, University of Nebraska Medical Center, Omaha, NE (C.R.H.).

Running Title Page

Running title: PK/PD relationship of RyR2 inhibitor *ent*-verticilide

Corresponding authors:

Björn C. Knollmann, M.D., Ph.D.

William Stokes Professor of Medicine and Pharmacology

Director, Vanderbilt Center for Arrhythmia Research and Therapeutics (VanCART)

Division of Clinical Pharmacology

Vanderbilt University School of Medicine

Medical Research Building IV, Rm. 1265

2215B Garland Ave

Nashville, TN 37232-0575

Office: (615) 343-6493 • Lab: (615) 936-7303 • Fax: (615) 343-0434

Email: bjorn.knollmann@vanderbilt.edu

Lab Url: <http://www.mc.vanderbilt.edu/knollmannlab>

Or

Jeffrey N. Johnston – Department of Chemistry & Vanderbilt Institute of Chemical Biology,

Vanderbilt University, Nashville, TN 37235-1822, USA;

Email: jeffrey.n.johnston@vanderbilt.edu

Or

Wendell S. Akers, Pharm.D., Ph.D.

Professor of Pharmacy and Pharmaceutical Sciences

Executive Director, Pharmaceutical Sciences Research Center

Associate Dean of Research

Lipscomb University College of Pharmacy

1 University Park Drive

Nashville, TN 37204

Email: scott.akers@lipscomb.edu

Number of text pages: 31

Number of tables: 1

Number of figures: 7

Number of references: 34

Number of words in the abstract: 238

Number of words in the introduction: 352

Number of words in the discussion: 1393

Non-standard Abbreviations:

AUC: area under the curve

C_{max}: maximum concentration

CPVT: catecholaminergic polymorphic ventricular tachycardia

E_{max}: maximum effect

IC₅₀: half-maximal inhibitory concentration

PD: pharmacodynamic

PK: pharmacokinetic

RYR2: cardiac ryanodine receptor

VEB: ventricular ectopic beat(s)

Recommended section assignment:

Cardiovascular

Abstract

The unnatural verticilide enantiomer (*ent*-verticilide) is a selective and potent inhibitor of cardiac ryanodine receptor (RyR2) calcium release channels and exhibits antiarrhythmic activity in a murine model of catecholaminergic polymorphic ventricular tachycardia (CPVT). To determine verticilide's pharmacokinetic and pharmacodynamic properties *in vivo*, we developed a bioassay to measure *nat*- and *ent*-verticilide in murine plasma and correlated plasma concentrations with antiarrhythmic efficacy in a mouse model of CPVT. *nat*-Verticilide rapidly degraded in plasma *in vitro*, showing >95% degradation within five minutes, whereas *ent*-verticilide showed <1% degradation over six hours. Plasma was collected from mice following intraperitoneal administration of *ent*-verticilide at two doses (3 mg/kg, 30 mg/kg). Peak plasma concentration (C_{\max}) and area under the plasma-concentration time curve (AUC) scaled proportionally to dose and the half-life was 6.9 hr for the 3 mg/kg dose and 6.4 hr for the 30 mg/kg dose. Antiarrhythmic efficacy was examined using a catecholamine challenge protocol at time points ranging from 5 to 1440 min after intraperitoneal dosing. *ent*-Verticilide inhibited ventricular arrhythmias as early as 7 min after administration in a concentration-dependent manner, with an estimated potency (IC_{50}) of 266 ng/mL (312 nM) and an estimated maximum inhibitory effect of 93.5%. Unlike the FDA-approved pan-RyR blocker dantrolene, the RyR2-selective blocker *ent*-verticilide (30 mg/kg) did not reduce skeletal muscle strength *in vivo*. We conclude that *ent*-verticilide has favorable pharmacokinetic properties and reduces ventricular arrhythmias with an estimated potency in the nanomolar range, warranting further drug development.

Significance Statement

ent-Verticilide has therapeutic potential to treat cardiac arrhythmias, but little is known about its pharmacological profile *in vivo*. The primary purpose of this study is to determine the systemic exposure and pharmacokinetics of *ent*-verticilide in mice and estimate its efficacy and potency *in vivo*. The current work suggests *ent*-verticilide has favorable pharmacokinetic properties and reduces ventricular arrhythmias with an estimated potency in the nanomolar range, warranting further drug development.

Introduction

The cardiac ryanodine receptor (RyR2) mediates contraction of the heart by releasing calcium from intracellular stores in response to electrical excitation (Bers, 2002). Untimely calcium release is a pathological mechanism that generates aberrant electrical activity, causing potentially fatal arrhythmias (Landstrom et al., 2017). Increased RyR2 activity can be caused by gene mutations in RyR2 or its regulatory binding proteins such as cardiac calsequestrin (Casq2), which cause a genetic arrhythmia syndrome characterized by stress- or exercise-induced ventricular arrhythmia, known as catecholaminergic polymorphic ventricular tachycardia (CPVT) (Wleklinski et al., 2020). Increased RyR2 activity has also been observed in other cardiac diseases associated with arrhythmias, such as atrial fibrillation (Voigt et al., 2012) and heart failure (Dobrev and Wehrens, 2014), among others. To date, there is no clinically approved RyR2-selective inhibitor. A non-selective ryanodine receptor inhibitor, dantrolene, is FDA-approved but causes muscle weakness due to block of RyR1, the ryanodine receptor expressed in skeletal muscle. Treatments targeted selectively to RyR2 could provide therapeutic benefit for patients with cardiac arrhythmias without causing skeletal muscle symptoms (Kansakar et al., 2021).

Recently, we discovered that the unnatural verticilide enantiomer (*ent*-verticilide) inhibits RyR2 *in vitro* with high potency but has no activity on skeletal RyR1 (Batiste et al., 2019). In contrast, the natural product (Shiomi et al., 2010) – *nat*-verticilide – did not inhibit RyR2 *in vitro*, demonstrating a rare, if not unprecedented, case where the non-natural mirror image of a natural product harbors all activity (Finefield et al., 2012). Moreover, *ent*-verticilide is composed of D-alanine and L- α -hydroxyheptanoic acid units (Heitz et al., 1989), leading to the hypothesis that the absolute configuration may be directly related to its *in vivo* exposure and duration of action (Lai et al., 2021). *ent*-Verticilide at a dose of 30 mg/kg had antiarrhythmic activity *in vivo* in a Casq2 knockout (Casq2^{-/-}) mouse model of CPVT, but its concentration dependence is not

known (Batiste et al., 2019). Given the broad interest in bioactive cyclic oligomeric depsipeptides (Süssmuth et al., 2011), the objective of our study was to determine *ent*-verticilide's *in vivo* pharmacokinetic/pharmacodynamic relationship as an antiarrhythmic agent in mice, and examine its effect on skeletal muscle function.

Materials and Methods

Drugs, chemicals, and reagents- Reference standards for *ent*-verticilide, *nat*-verticilide, and deuterated *ent*-verticilide (internal standard) were synthesized with a purity of >95% (Supp. Materials and Methods). Drug-free mouse plasma was purchased from BioIVT (Westbury, NY). Liquid chromatography mass spectrometry (LCMS) grade acetonitrile and formic acid were purchased from Thermo Fisher Scientific (Pittsburgh, PA). LC/MS grade water was prepared by a Milli-Q-ultrapure water system (Burlington, MA).

Synthesis – See supporting information (Supp. Experimental Procedures and Characterization Data for Reported Compounds) for detailed synthetic procedures and spectral data (Supp. Figures 1 – 3).

Plasma and whole blood stability experiments- Drug-free mouse plasma was preincubated in polypropylene microcentrifuge tubes for 30 minutes at 4 °C or on a microplate shaker at 37 °C prior to the addition of *ent*-verticilide or *nat*-verticilide (final concentration 2500 ng/mL). Following a 5-minute equilibration period after drug addition to microcentrifuge tubes, 20 µL of plasma was removed at 0, 30, 60, 120, 240 and 360 minutes to evaluate compound stability in mouse plasma. Samples were transferred to a 96-well polypropylene plate containing 250 µL of ice-cold acetonitrile containing *ent*-verticilide-*d*₁₂ (100 ng/mL). Samples were mixed multiple times with a pipette to ensure precipitation of plasma proteins and the plate was covered with an adhesive film to prevent solvent evaporation. Samples remained on ice throughout the experiment until the last sample collection time point. The plate was centrifuged at 4800 rpm for 10 minutes and 200 µL of supernatant was transferred to a new 96 deep well polypropylene deep well plate, evaporated under a stream of nitrogen gas, and reconstituted with 125 µL of mobile phase prior to LCMS analysis. For whole blood stability testing, *ent*-verticilide (final concentration 2500 ng/mL) was added to fresh mouse whole blood (1.5 mL) containing EDTA

and allowed to equilibrate for 30 minutes on a microplate shaker (250 rpm) at 37 °C. After the preincubation period, 200 µL of whole blood were removed at 0, 30, 60, 120, 240, and 360 minutes and centrifuged at 2500 rpm to obtain plasma. Plasma (100 µL) was transferred to a 96-well protein precipitation plate containing 300 µL of ice-cold acetonitrile containing *ent*-verticilide-*d*₁₂ (100 ng/mL). Samples were filtered using a positive pressure manifold and the filtrate was transferred to a new 96 deep well polypropylene deep well plate, evaporated under a stream of nitrogen gas, and reconstituted with 125 µL of mobile phase prior to LCMS analysis. Peak area ratios of the analyte and internal standard for each plasma sample were analyzed by liquid chromatography coupled to tandem mass spectrometry (LC-MS/MS) and normalized to the area ratio for time point 0 (baseline) to calculate the percent of *ent*-verticilide and *nat*-verticilide remaining at each time point. Criteria for establishing compound stability was set at 90% and 80% remaining at 60 and 120 minutes, respectively.

Whole blood to plasma ratio- Aliquots of fresh whole blood and control plasma (separated from fresh whole blood in parallel) from mice were spiked with *ent*-verticilide (final concentration 2500 ng/ml) and then incubated at 37 °C for 30 minutes. After completion of the incubation period, plasma was separated from whole blood samples by centrifugation at 2500 rpm for 20 minutes. Four 50 µl aliquots of each sample (plasma isolated from whole blood and control plasma) were transferred to a protein precipitation plate (Phenomenex, Torrance, CA) containing 300 µ L of ice-cold acetonitrile spiked with internal standard (*ent*-verticilide-*d*₁₂; 100 ng/mL). Samples were mixed using a single-channel pipette, eluted into a clean 96-well plate using a positive pressure manifold, concentrated under a stream of nitrogen gas at 40 °C, and reconstituted with 90:10 (v/v) 0.1% formic acid in water:acetonitrile prior to LC-MS/MS analysis. The blood to plasma ratio (B/P ratio) of *ent*-verticilide was calculated using following equation:

$$B/P\ ratio = \frac{C_{cp}}{C_{wbp}}$$

Where, C_{cp} is the concentration of *ent*-verticilide in control plasma sample and C_{wbp} is the concentration *ent*-verticilide in plasma separated from whole blood samples.

LC-MS/MS analysis of verticilide- Detection of *ent*-verticilide, *nat*-verticilide, and *ent*-verticilide- d_{12} was carried out using LC-MS/MS with electrospray ionization set in the positive ion mode followed by multiple-reaction monitoring of precursor and product ions for each analyte: *ent*-verticilide (m/z 853.6 to 214.1), *nat*-verticilide (m/z 853.6 to 214.1), and *ent*-verticilide- d_{12} (m/z 865.9 to 216.9). Quantification of *ent*-verticilide in plasma was qualified using eight standards (2.5 – 5000 ng/mL) and three quality control levels (30, 300, 3000 ng/mL) prepared in blank mouse plasma. Plasma samples from the pharmacokinetic study in mice were thawed at room temperature and 100 μ L was transferred to a protein precipitation plate (Phenomenex, Torrance, CA) containing 300 μ L of ice-cold acetonitrile spiked with internal standard (*ent*-verticilide- d_{12} ; 100 ng/mL). Samples were mixed using a multichannel pipette, eluted into a clean 96-well plate using a positive pressure manifold, concentrated under a stream of nitrogen gas at 40 °C, and reconstituted with 90:10 (v/v) 0.1% formic acid in water:acetonitrile. Samples were loaded into a CTC Analytics PAL-xt DW autosampler and 5 μ L was injected into a Shimadzu LC-20 AD Series HPLC System coupled to a Sciex 6500 QTrap mass spectrometer (Foster City, CA). Analytes were separated on a C-18 column (50 \times 2.1 mm, 1.7 μ m, Phenomenex, Torrance, CA) heated to 60 °C using a 90:10 (v/v) mobile phase mixture of 0.1% formic acid in water (mobile phase A) and 0.1% formic acid in acetonitrile (mobile phase B) at a flow rate of 0.5 mL/min. The gradient for mobile phase B was increased from 5 to 90% over 0.5 minutes with a total run time of 2.5 minutes. All standards and quality control samples met the following acceptance criteria: (1) standard curve of at least 5 standards each within 15% of the nominal concentration and an $R^2 > 0.90$; (2) 66.7% of all QC samples and at least 50% at each QC level (low, medium, and high) were within 15% of the nominal concentration. Mouse

samples with *ent*-verticilide plasma concentrations that exceeded the high end of the standard curve were diluted 1:10 or 1:100 with blank mouse plasma, recalculated using a dilution factor of 10 or 100, and were accepted if the corresponding diluted QC met the above QC criteria.

Pharmacokinetic analysis- Mouse plasma concentrations of *ent*-verticilide at each time point were imported into Phoenix WinNonlin® 8.0 software (Certara USA, Inc., Princeton, NJ) and underwent noncompartmental pharmacokinetic analysis using Model 200 (Plasma; Single Extravascular Dose; Linear Log Trapezoidal Method). A sparse sampling approach was used to estimate the maximum observed plasma concentration (C_{max}), time to the maximum observed plasma concentration (T_{max}), the area under the concentration-time curve from zero to infinity (AUC_{inf}), and the half-life ($T_{1/2}$). Extravascular volume of distribution (V_d/F) and clearance (Cl/F) for *ent*-verticilide was estimated by noncompartmental analysis and normalized to animal body weight (mg/kg).

In vivo study design- Mice were housed by the Vanderbilt Division of Animal Care with unrestricted access to water and food. All procedures and protocols were approved by the Institutional Animal Care and Use Committee (IACUC protocol #M1900057). Prior to carrying out the study, it was determined that two doses (3 and 30 mg/kg drug/body weight) would be tested, with at least 1 male and 1 female mouse sampled at each dose and time. Sixty-six *Casq2*^{-/-} mice (34 males and 32 females) 12-14 weeks old were used as available (Supp. Figure 4). Initially, plasma samples were collected out to 480 minutes. However, after measuring plasma concentration levels during the study, it was decided that additional 960- and 1440-minute time points be added to the 30 mg/kg dose group to give a complete plasma concentration profile. During the study one mouse bled during intraperitoneal administration of *ent*-verticilide and was excluded from plasma collection (not counted in the above numbers).

Skeletal muscle force measurements- Mice were anesthetized with inhaled isoflurane (2%) while breathing spontaneously and placed prone on a heating pad at 37 °C. Needle electrodes were placed 1 cm apart in the sciatic notch and were stimulated with five trains of 15 pulses of 5 ms, 10 mA to induce repeated contraction of the gastrocnemius muscle. Muscle force was measured with a force transducer (AD Instruments) placed over the left hind paw. Stimulated pulses and recordings were acquired using PowerLab 26T (AD Instruments) and analyzed using LabChart Pro 4 software (AD Instruments).

Electrocardiogram recording- To establish a baseline of ventricular arrhythmia for each mouse, mice were manually restrained using the one-handed method (Machholz et al., 2012), injected intraperitoneally with vehicle (10% DMSO + saline; 13.1 mL/kg) using a 25-gauge needle, and returned to their cage for 30 minutes. Mice were then anesthetized with inhaled isoflurane titrated to the lowest possible level (~1.3%) and anesthetic effect confirmed by lack of pedal withdrawal reflex. Upon establishing stable anesthesia, four limb needle electrodes were placed to generate electrocardiogram (ECG) leads I and II, and a stable baseline heart rate was established (~1 minute). Anesthetized mice were injected intraperitoneally (right side) with 3.0 mg/kg isoproterenol and ECGs recorded for an additional two minutes, before being returned to their cages.

Seven days later, anesthetized (5-minute group) or conscious mice (all other time points) were manually restrained and *ent*-verticilide (3 or 30 mg/kg; in 10% DMSO + saline; 13.1 mL/kg) was administered intraperitoneally (left side) with a 25-gauge needle at 5 (unconscious), 10, 15, 30, 60, 120, 240, 480, 960, or 1440 minutes (conscious) before plasma collection. Mice were monitored for pain or distress (none exhibited) and then anesthetized with inhaled isoflurane approximately 5 minutes before the indicated time points. The above catecholamine administration (right side) was then repeated. It was necessary to anesthetize the 5-minute time group prior to administration of *ent*-verticilide to give enough time to collect ECG recordings

(approximately 2 minutes) before the blood draw. An independent second set of 31 mice were used to examine the week-to-week variation in the arrhythmia response. Mice were treated with vehicle at baseline, as described above, and then one week later again with vehicle (instead of *ent*-verticilide) before the arrhythmia challenge.

Plasma collection- At the completion of ECG recording, isoflurane was titrated to 3%, a thoracotomy was performed, and whole blood was drawn by left ventricular cardiac puncture using an EDTA-coated 21-gauge needle. The beginning of the blood draw was timed to coincide with the time points listed above and took approximately 60 seconds, hence ECG records were obtained for each mouse approximately three minutes prior to blood collection. Whole blood was immediately centrifuged at 500 gravity for 10 minutes at 4 °C and the supernatant stored at -80 °C until analysis.

ECG analysis- ECG recordings were analyzed using LabChart (AD Instruments) by an individual blinded to the treatment dose and time. All ventricular ectopic beats (VEB) were counted; couplets were defined as two consecutive VEB and ventricular tachycardia was defined as three or more consecutive VEB. To quantify the degree of antiarrhythmic effect of *ent*-verticilide, we only included mice that exhibited a significant ventricular arrhythmia burden (>25 ventricular ectopic beats, VEB) during the baseline catecholamine challenge. 53 out of 66 mice (80.3%) fulfilled the inclusion criteria and were used to estimate the *ent*-verticilide concentration-effect relationship.

Statistics and pharmacodynamic modeling- All statistics were carried out in GraphPad Prism (v9.4.1) and are indicated in the figure legends and in detail in Supp. Table 1. Linear regression was used to model heart rate vs plasma concentration with the equation: $Y = Y_{\text{Intercept}} + \text{Slope} \times X$ using least squares regression, no weighting, and no constraints on the parameters.

Nonlinear regression was used to model VEB vs plasma concentration data with the equation:
$$Y = \text{Bottom} + (\text{Top} - \text{Bottom}) / (1 + (\text{IC}_{50}/X)^{\text{HillSlope}})$$
 using least squares regression, no weighting, and no constraints on the parameters.

Results

ent- And nat-verticilide plasma stability in vitro

After establishing bioassays for both *ent-* and *nat*-verticilide (Figure 1A), we first measured drug stability in mouse plasma. *ent*-Verticilide was stable at both 4 and 37 °C in mouse plasma for up to 6 hours (Figure 1B, C), as well as whole blood (Figure 1D). The blood to plasma ratio of *ent*-verticilide in mice was estimated to be approximately 0.85 and indicates that *ent*-verticilide does not readily accumulate in red blood cells relative to plasma. *nat*-Verticilide, however, underwent immediate degradation in mouse plasma at both 4 and 37 °C and was no longer detectable at 30 minutes (Figure 1B, C).

ent-Verticilide antiarrhythmic efficacy in vivo

To study the pharmacokinetic and pharmacodynamic properties of *ent*-verticilide *in vivo*, we utilized a mouse model of severe CPVT, *Casq2*^{-/-} mice (Knollmann et al., 2006). Arrhythmia burden was assessed by electrocardiography (ECG) during a two-minute period following catecholamine challenge (isoproterenol 3.0 mg/kg intraperitoneal) under isoflurane anesthesia, a well-established protocol that elicits ventricular arrhythmia in the majority of *Casq2*^{-/-} mice. To correlate *ent*-verticilide plasma concentration with its antiarrhythmic effect, we devised the following protocol (Figure 2A): All mice underwent a catecholamine challenge protocol at baseline and one week later after *ent*-verticilide treatment. Plasma was collected immediately after the second catecholamine challenge protocol by cardiac puncture. Prior to the second catecholamine challenge, we administered *ent*-verticilide at times points ranging from 5 min to 1440 min before plasma collection. Using the protocol shown in Figure 2A, we tested two doses: 30 mg/kg, the dose used in our previous report, and a 10-fold lower dose (3 mg/kg).

Representative heart rate responses and example ECG records are shown in Figure 2B and 2C. Both doses of *ent*-verticilide significantly reduced the amount and severity of the ventricular arrhythmia in *Casq2*^{-/-} mice (Figure 2D). In aggregate, mice treated with *ent*-verticilide exhibited

significantly lower rates of ventricular ectopy and VT duration compared to the baseline catecholamine challenge (Figure 2E). In contrast, an independent set of 31 *Casq2*^{-/-} mice had a modest increase in VEB (median = 149 vs 205, $p = 0.080$) and no change in VT duration ($p = 0.89$) when treated with vehicle one week after baseline (Supp. Figure 5).

ent-Verticilide pharmacokinetic properties

We first determined systemic exposure of a 3 mg/kg and 30 mg/kg dose of *ent*-verticilide following intraperitoneal administration in mice. *ent*-Verticilide was rapidly absorbed following intraperitoneal injection and displayed multicompartmental kinetics with a rapid distribution phase followed by a slower elimination phase (Figure 3A, B). Systemic exposure was dose-dependent but there were no differences in plasma concentrations between male and female mice (Supp. Figure 6). Noncompartmental pharmacokinetic estimates of *ent*-verticilide are reported in Table 1. A dose-proportional increase in C_{\max} and AUC_{inf} was observed following a 3 mg/kg and 30 mg/kg dose of *ent*-verticilide with an elimination half-life of 6.92 hours and 6.37 hours, respectively. The extravascular volume of distribution and systemic clearance was approximately 21% and 15% lower in the 30 mg/kg dose compared to the 3 mg/kg dose.

ent-Verticilide pharmacokinetic-pharmacodynamic relationship as antiarrhythmic agent

To establish a relationship between plasma concentration and antiarrhythmic efficacy, we calculated, for each mouse that exhibited robust ventricular arrhythmias at baseline, the percent change in arrhythmia burden – measured as number of VEBs – between the baseline catecholamine challenge and the catecholamine challenge after *ent*-verticilide treatment. Elevated *ent*-verticilide concentrations in the plasma were associated with a reduction in VEBs (Figure 3C & 3D). RyR2-mediated calcium release contributes to the pacemaking activity of the sinoatrial node (Hata et al., 1996; Rigg and Terrar, 1996), and RyR2 block by *ent*-verticilide is known to significantly reduce sinus heart rates during catecholamine challenge (Batiste et al.,

2019). Hence, we examined the effect of *ent*-verticilide on basal and peak heart rate during the catecholamine challenge protocol (Figure 4). While, in aggregate, both doses of *ent*-verticilide significantly reduced basal and peak heart rate (Figure 4A & 4C), there was no significant concentration-response relationship (Figure 4B & 4D). Next, we examined the concentration-response data for any lag in therapeutic response. The average inhibitory effect of *ent*-verticilide was plotted together with the plasma concentration over the first 30 min (Figure 5). Except for the first time point (5 min), *ent*-verticilide plasma levels were closely correlated with the inhibition of ventricular ectopy for both doses (Figure 5A & 5B). The lag of response is also evident in the counter-clockwise hysteresis of the concentration-effect relationship (Figure 5C & 5D). Note that ECGs were recorded approximately 3 min before plasma collection. Hence, the arrhythmia assessment for the 5 min plasma collection occurred 2 minutes after *ent*-verticilide administration, and for the 10 min plasma collection it was 7 min after *ent*-verticilide administration. As such, the onset of *ent*-verticilide's antiarrhythmic activity is rapid, occurring between 2 min and 7 min after drug administration. Given that hysteresis was minimal and that, except for the 5-minute data point, plasma concentrations were closely correlated with antiarrhythmic efficacy, we combined data from all mice, leaving out the 5-minute time point, and constructed a concentration-response relationship to estimate the potency and efficacy of *ent*-verticilide *in vivo* (Figure 6). The estimate for 50% inhibitory concentration (IC_{50}) is 266 ng/mL (312 nM) and the estimate for maximum inhibitory effect (E_{max}) is 93.5%.

ent-Verticilide's effect on skeletal muscle function

To determine whether *ent*-verticilide inhibits the skeletal muscle RyR isoform (RyR1) *in vivo*, we treated 18 mice (6 per group) with vehicle, 30 mg/kg *ent*-verticilide, or 20 mg/kg dantrolene (i.p.). Dantrolene is a potent inhibitor of RyR1. Hind-limb muscle force measurements were collected from anesthetized mice using programmed electrical stimulation of the sciatic notch before administration and 5, 10, and 15 minutes after drug administration. Dantrolene, but not

vehicle or *ent*-verticilide, reduced the muscle force at 5, 10, and 15 minutes, relative to baseline (Figure 7). There were no differences between *ent*-verticilide and vehicle. As such, even at the high dose tested – and at time points coinciding with arrhythmia suppression where plasma concentrations were highest – *ent*-verticilide did not impair skeletal muscle function, demonstrating selectivity for cardiac RyR2 over skeletal RyR1 *in vivo*.

Discussion

The goal of our study was to evaluate the pharmacokinetic and pharmacodynamic properties of *ent*-verticilide as an antiarrhythmic agent and determine whether *ent*-verticilide has off-target effects on skeletal muscle function. We find that (1), *ent*-verticilide is stable in plasma and readily absorbed after subcutaneous administration, (2) has favorable pharmacokinetic properties with a half-life of 3-6 hours, (3) is effective *in vivo* as an antiarrhythmic agent with an estimated potency in the nanomolar range, and (4), does not cause skeletal muscle weakness unlike the clinically-available pan-RyR blocker dantrolene.

Plasma stability- One key finding from the present study is the biological stability and extravascular absorption of the unnatural enantiomer, *ent*-verticilide. Both peptide cyclization and the incorporation of non-natural amino acids are common strategies used in lead development to overcome high rates of proteolytic degradation or poor membrane permeability of therapeutic peptides (Adessi and Soto, 2002; Bird et al., 2010; Diao and Meibohm, 2013; Henninot et al., 2018; Buckton et al., 2021). Unlike the rapid *in vitro* degradation of *nat*-verticilide, *ent*-verticilide was stable in mouse plasma for several hours. This suggests that the configuration at key proteolytic sites within the structure of *ent*-verticilide imparts enhanced metabolic stability against plasma proteases. This is not unexpected since the α -amino ester configuration is epimeric to natural α -amino acids, and the activity of plasma proteases and esterases is configurationally dependent (Diao and Meibohm, 2013; Nielsen et al., 2017; Buckton et al., 2021). Incorporation of non-natural amino acid stereochemistry throughout the backbone structure of *ent*-verticilide could also facilitate other intramolecular interactions within the ring structure to impair protease access to key proteolytic sites within the cyclic oligomeric depsipeptide (Diao and Meibohm, 2013).

Pharmacokinetics- Recent reports indicate that cyclization of peptides and their stereochemistry have a significant impact on membrane permeability and bioavailability of therapeutic proteins (Rand et al., 2012; Jwad et al., 2020; Buckton et al., 2021; Caron et al., 2021). We used intraperitoneal administration to avoid degradation pathways within the gastrointestinal tract and serve as a proof-of-concept study to evaluate *in vivo* drug exposure and target engagement of *ent*-verticilide in our preclinical ventricular arrhythmia animal model. Results from our *in vivo* pharmacokinetic study demonstrate that *ent*-verticilide is rapidly absorbed from the peritoneal cavity into the systemic circulation. Although the impact of pre-systemic proteolytic activity and first-pass metabolism on the absolute bioavailability of *ent*-verticilide was not evaluated here, systemic peptide levels were sufficient for target engagement in both the low and high dose treatment groups. Thus, the enhanced *in vitro* biological stability to proteases translated to *in vivo* bioavailability and systemic exposure of *ent*-verticilide, as has been reported for other cyclic depsipeptides (Rand et al., 2012; Nielsen et al., 2017).

Evaluation of *ent*-verticilide plasma concentration versus time profiles and exposure data at each dose demonstrated a dose-proportional increase in the extent of absorption (AUC and C_{max}) with a similar rate of absorption (T_{max}). Although the extravascular volume of distribution and systemic clearance was slightly lower for the 30 mg/kg dose, both had a similar elimination half-life of 6.92 hours and 6.37 hours for the 3 mg/kg and 30 mg/kg doses, respectively. Although the absolute bioavailability of *ent*-verticilide is unknown following intraperitoneal administration, the estimated 15% higher relative bioavailability for the 30 mg/kg dose compared to the 3 mg/kg dose could account for a large percentage of the difference between the extravascular volume of distribution and systemic clearance estimates between the two doses. The high extravascular volume of distribution suggests extensive tissue distribution relative to the circulating blood volume for mice (Diehl et al., 2001). Given its prolonged *in vitro* stability in mouse plasma, the *in vivo* clearance estimate of *ent*-verticilide is likely attributed to either hepatic drug metabolism enzymes, extrahepatic proteases, or renal clearance mechanisms.

Collectively, these pharmacokinetic data suggest *ent*-verticilide demonstrates linear kinetics over the extravascular dose range of 3 – 30 mg/kg with an elimination half-life sufficient to support dosing strategies required for both acute and chronic drug exposures in preclinical models as *in vivo* pharmacological tool or therapeutic agent.

Target engagement- Both the low and high dose *ent*-verticilide treatment groups produced sufficient *in vivo* target engagement at RyR2 to suppress VEB. Importantly, *ent*-verticilide was selective for RyR2, having no inhibition of the skeletal muscle isoform RyR1. The pharmacodynamic counter-clockwise hysteresis observed following intraperitoneal administration of *ent*-verticilide is likely attributed to a distributional delay between systemic drug concentrations and the time to target engagement with RyR2 in cardiac muscle. The brief temporal delay in VEB inhibition within the first 5-10 minutes of *ent*-verticilide administration is consistent with the time it would take to achieve tissue equilibrium in a highly perfused organ such as the myocardium (Sundberg et al., 1998). Previous myocardial uptake studies in humans and preclinical animal models have demonstrated this type of counterclockwise hysteresis loop for other drugs with their site of action in the heart (Louizos et al., 2014). After 5-10 minutes when tissue equilibrium within the myocardium is presumed to have been achieved, VEB suppression correlated with plasma *ent*-verticilide concentrations throughout the pharmacokinetic elimination phase. Redistribution of *ent*-verticilide from peripheral compartments back into the systemic circulation to maintain higher plasma concentrations may have contributed to the persistent pharmacodynamic effect observed in the high-dose group (90% inhibition) versus the low-dose group at 60 minutes (0% inhibition).

Utility as antiarrhythmic agent in vivo- We find that *ent*-verticilide inhibited ventricular arrhythmias as early as 7 min after administration in a concentration-dependent manner, with an estimated potency (IC₅₀) of 266 ng/mL and an estimated maximum inhibitory effect of 93.5%.

These data compare favorably with antiarrhythmic agents currently approved for clinical use. For example, the class Ia and Ic antiarrhythmic drugs procainamide, quinidine and lidocaine are less potent *in vivo*, requiring 10-fold higher plasma concentrations for therapeutic efficacy (therapeutic trough concentrations of 2000 – 8000 ng/ml) (Brunton and Knollmann, 2023). *ent*-Verticilide is comparable in potency to the class Ic agents flecainide and propafenone (therapeutic trough concentrations of 200 – 1000 ng/ml) (Brunton and Knollmann, 2023). However, both flecainide and propafenone have liability for fatal arrhythmias due to their sodium channel block (Knollmann and Roden, 2008), whereas *ent*-verticilide does not block sodium channels (Batiste et al., 2019). As such, *ent*-verticilide could be much safer than antiarrhythmic drugs currently approved for clinical use.

Limitations- A limitation and potential source of bias of our study is that our antiarrhythmic efficacy estimate was based on the difference between ventricular ectopy at baseline and one week later after *ent*-verticilide administration. Any time-dependent reduction in the rate of ventricular arrhythmia during the second catecholamine challenge would bias the results towards overestimating the antiarrhythmic efficacy. However, the ventricular ectopy burden was not significantly different between the two catecholamine challenges in a relatively large number of mice (n=31) that received two vehicle treatments (see Supp. Figure 5), supporting the validity of the efficacy estimates used in our PK-PD analysis (Figure 6).

Other limitations include that dose-dependent systemic exposure of *ent*-verticilide was measured following intraperitoneal administration and that pharmacokinetic parameters were estimated utilizing a sparse sampling approach (Peng et al., 2009). This approach relies on a single blood sample from individual animals at different times points following drug administration and pools individual animal levels to provide a population pharmacokinetic parameter estimate. Future dose-ranging studies in larger preclinical animal models with alternative routes of administration will utilize more intensive serial blood sampling approaches

within individual animals to further characterize the pharmacokinetic properties (absolute bioavailability, systemic volume of distribution and clearance) of *ent*-verticilide and refine its pharmacokinetic/pharmacodynamic relationship to inhibit cardiac arrhythmias. Nonetheless, the data provide good agreement between plasma concentration and antiarrhythmic efficacy.

Final considerations- Results from this study extend our previous *in vitro* concentration-response analysis from cardiomyocytes (Batiste et al., 2019) to mice *in vivo*, and demonstrate the favorable pharmacokinetic properties and potential use of *ent*-verticilide as an *in vivo* pharmacological tool to treat cardiac arrhythmias. Importantly, our study supports the proof of concept that the cyclic oligomeric depsipeptide *ent*-verticilide is rapidly absorbed following intraperitoneal administration and produces sufficient *in vivo* target engagement to suppress ventricular arrhythmias with a potency in the nanomolar range. This finding, along with the excellent *in vitro* stability profile of *ent*-verticilide, supports the use of plasma as the biologic matrix to characterize the *in vivo* exposure of *ent*-verticilide in preclinical and clinical studies. Future *in vitro* studies will need to explore potential biotransformation pathways and metabolites of *ent*-verticilide along with preformulation analysis to support drug delivery strategies.

Acknowledgements

None.

Data Availability Statement

The authors declare that all the data supporting the findings of this study are available within the paper and its Supplemental Data

Authorship Contributions

Participated in research design: Blackwell, Smith, Hopkins, Akers, Johnston, and Knollmann.

Conducted experiments: Blackwell, Smith, Do, Gochman, Schmeckpeper, and Akers.

Performed data analysis: Blackwell, Smith, Do, Gochman, Schmeckpeper, and Akers.

Wrote or contributed to writing of the manuscript: Blackwell, Smith, Do, Hopkins,

Schmeckpeper, Akers, Johnston, and Knollmann.

References

- Adessi C and Soto C (2002) Converting a peptide into a drug: strategies to improve stability and bioavailability. *Curr Med Chem* **9**:963-978.
- Batiste SM, Blackwell DJ, Kim K, Kryshtal DO, Gomez-Hurtado N, Rebbeck RT, Cornea RL, Johnston JN and Knollmann BC (2019) Unnatural verticilide enantiomer inhibits type 2 ryanodine receptor-mediated calcium leak and is antiarrhythmic. *Proc Natl Acad Sci U S A* **116**:4810-4815.
- Bers DM (2002) Cardiac excitation-contraction coupling. *Nature* **415**:198-205.
- Bird GH, Madani N, Perry AF, Princiotta AM, Supko JG, He X, Gavathiotis E, Sodroski JG and Walensky LD (2010) Hydrocarbon double-stapling remedies the proteolytic instability of a lengthy peptide therapeutic. *Proc Natl Acad Sci U S A* **107**:14093-14098.
- Brunton L and Knollmann B (2023) *Goodman & Gilman's the Pharmacological Basis of Therapeutics*. McGraw Hill Medical, New York, NY.
- Buckton LK, Rahimi MN and McAlpine SR (2021) Cyclic Peptides as Drugs for Intracellular Targets: The Next Frontier in Peptide Therapeutic Development. *Chemistry* **27**:1487-1513.
- Caron G, Kihlberg J, Goetz G, Ratkova E, Poongavanam V and Ermondi G (2021) Steering New Drug Discovery Campaigns: Permeability, Solubility, and Physicochemical Properties in the bRo5 Chemical Space. *ACS Med Chem Lett* **12**:13-23.
- Diao L and Meibohm B (2013) Pharmacokinetics and pharmacokinetic-pharmacodynamic correlations of therapeutic peptides. *Clin Pharmacokinet* **52**:855-868.
- Diehl KH, Hull R, Morton D, Pfister R, Rabemampianina Y, Smith D, Vidal JM, van de Vorstenbosch C and Methods EFoPIAaECftVoA (2001) A good practice guide to the administration of substances and removal of blood, including routes and volumes. *J Appl Toxicol* **21**:15-23.

- Dobrev D and Wehrens XH (2014) Role of RyR2 phosphorylation in heart failure and arrhythmias: Controversies around ryanodine receptor phosphorylation in cardiac disease. *Circ Res* **114**:1311-1319; discussion 1319.
- Finefield JM, Sherman DH, Kreitman M and Williams RM (2012) Enantiomeric natural products: occurrence and biogenesis. *Angew Chem Int Ed Engl* **51**:4802-4836.
- Hata T, Noda T, Nishimura M and Watanabe Y (1996) The role of Ca²⁺ release from sarcoplasmic reticulum in the regulation of sinoatrial node automaticity. *Heart Vessels* **11**:234-241.
- Heitz F, Kaddari F, Heitz A, Raniriseheno H and Lazaro R (1989) Conformations, cation binding, and transmembrane ion transfer properties of a cyclooctapeptide built by an alternation of D and L residues. *Int J Pept Protein Res* **34**:387-393.
- Henninot A, Collins JC and Nuss JM (2018) The Current State of Peptide Drug Discovery: Back to the Future? *J Med Chem* **61**:1382-1414.
- Jwad R, Weissberger D and Hunter L (2020) Strategies for Fine-Tuning the Conformations of Cyclic Peptides. *Chem Rev* **120**:9743-9789.
- Kansakar U, Varzideh F, Jankauskas SS, Gambardella J, Trimarco B and Santulli G (2021) Advances in the understanding of excitation-contraction coupling: the pulsing quest for drugs against heart failure and arrhythmias. *Eur Heart J Cardiovasc Pharmacother* **7**:e91-e93.
- Knollmann BC, Chopra N, Hlaing T, Akin B, Yang T, Ettensohn K, Knollmann BE, Horton KD, Weissman NJ, Holinstat I, Zhang W, Roden DM, Jones LR, Franzini-Armstrong C and Pfeifer K (2006) Casq2 deletion causes sarcoplasmic reticulum volume increase, premature Ca²⁺ release, and catecholaminergic polymorphic ventricular tachycardia. *J Clin Invest* **116**:2510-2520.
- Knollmann BC and Roden DM (2008) A genetic framework for improving arrhythmia therapy. *Nature* **451**:929-936.

- Lai X, Tang J and ElSayed MEH (2021) Recent advances in proteolytic stability for peptide, protein, and antibody drug discovery. *Expert Opin Drug Discov* **16**:1467-1482.
- Landstrom AP, Dobrev D and Wehrens XHT (2017) Calcium Signaling and Cardiac Arrhythmias. *Circ Res* **120**:1969-1993.
- Louizos C, Yáñez JA, Forrest ML and Davies NM (2014) Understanding the hysteresis loop conundrum in pharmacokinetic/pharmacodynamic relationships. *J Pharm Pharm Sci* **17**:34-91.
- Machholz E, Mulder G, Ruiz C, Corning BF and Pritchett-Corning KR (2012) Manual restraint and common compound administration routes in mice and rats. *J Vis Exp*.
- Nielsen DS, Shepherd NE, Xu W, Lucke AJ, Stoermer MJ and Fairlie DP (2017) Orally Absorbed Cyclic Peptides. *Chem Rev* **117**:8094-8128.
- Peng SX, Rockafellow BA, Skedzielewski TM, Huebert ND and Hageman W (2009) Improved pharmacokinetic and bioavailability support of drug discovery using serial blood sampling in mice. *J Pharm Sci* **98**:1877-1884.
- Rand AC, Leung SS, Eng H, Rotter CJ, Sharma R, Kalgutkar AS, Zhang Y, Varma MV, Farley KA, Khunte B, Limberakis C, Price DA, Liras S, Mathiowetz AM, Jacobson MP and Lokey RS (2012) Optimizing PK properties of cyclic peptides: the effect of side chain substitutions on permeability and clearance(). *Medchemcomm* **3**:1282-1289.
- Rigg L and Terrar DA (1996) Possible role of calcium release from the sarcoplasmic reticulum in pacemaking in guinea-pig sino-atrial node. *Exp Physiol* **81**:877-880.
- Shiomi K, Matsui R, Kakei A, Yamaguchi Y, Masuma R, Hatano H, Arai N, Isozaki M, Tanaka H, Kobayashi S, Turberg A and Omura S (2010) Verticilide, a new ryanodine-binding inhibitor, produced by *Verticillium* sp. FKI-1033. *J Antibiot (Tokyo)* **63**:77-82.
- Sundberg S, Antila S, Scheinin H, Häyhä M, Virtanen M and Lehtonen L (1998) Integrated pharmacokinetics and pharmacodynamics of the novel calcium sensitizer levosimendan as assessed by systolic time intervals. *Int J Clin Pharmacol Ther* **36**:629-635.

Süssmuth R, Müller J, von Döhren H and Molnár I (2011) Fungal cyclooligomer depsipeptides: from classical biochemistry to combinatorial biosynthesis. *Nat Prod Rep* **28**:99-124.

Voigt N, Li N, Wang Q, Wang W, Trafford AW, Abu-Taha I, Sun Q, Wieland T, Ravens U, Nattel S, Wehrens XH and Dobrev D (2012) Enhanced sarcoplasmic reticulum Ca²⁺ leak and increased Na⁺-Ca²⁺ exchanger function underlie delayed afterdepolarizations in patients with chronic atrial fibrillation. *Circulation* **125**:2059-2070.

Wleklinski MJ, Kannankeril PJ and Knollmann BC (2020) Molecular and tissue mechanisms of catecholaminergic polymorphic ventricular tachycardia. *J Physiol* **598**:2817-2834.

Footnotes

This research was supported in part by the National Institutes of Health National Heart, Lung, and Blood Institute [R35 HL144980 (to B.C.K.), R01 HL151223 (to J.N.J., B.C.K.), R31 HL151125 (to A.N.S.)]; the PhRMA Foundation Postdoctoral Fellowship (D.J.B.); the American Heart Association Arrhythmia and Sudden Death Strategically Focused Research Network grant [19SFRN34830019 (to B.C.K., W.S.A.)]; and the Leducq Foundation grant [18CVD05 (to B.C.K.)].

No author has an actual or perceived conflict of interest with the contents of this article.

Figure Legends

Figure 1. *ent*-Verticilide and *nat*-verticilide stability in murine plasma and whole blood. **A.**

Chemical structures for *nat*- and *ent*-verticilide. **B.** *ent*-Verticilide or *nat*-verticilide *in vitro* stability (% remaining) measured in plasma incubated at 4 °C or, **C.**, 37 °C. N = 4 replicates per drug per time point in B and C. Individual points shown alongside mean value connecting lines. **D.** *ent*-Verticilide *in vitro* stability measured in whole blood incubated at 37 °C. N = 1 per time point.

Figure 2. *ent*-Verticilide (*ent*-Vert) administration in a murine model of catecholaminergic

polymorphic ventricular tachycardia (*Casq2*^{-/-}). **A.** Study design for arrhythmia response and plasma collection. *Casq2*^{-/-} mice were treated with vehicle (DMSO) 30 minutes before recording electrocardiograms (ECG) with isoproterenol (iso) challenge to establish baseline measurements for pharmacodynamic response (blue). One week later, mice were treated with 3 or 30 mg/kg *ent*-Vert between 5 and 1440 minutes before recording ECGs during iso challenge and collecting plasma (red, study endpoint). **B.** Representative trace of the heart rate before and after iso administration (arrow, time = 0) in mice treated with vehicle or *ent*-Vert. The fluctuating heart rate is caused by beat-to-beat variation in the RR interval. **C.** Examples of electrocardiogram (ECG) recordings showing stable sinus rhythms before and after iso, and ventricular arrhythmias in the form of ventricular ectopic beats (VEB, *) or ventricular tachycardia (VT). **D.** Incidence of arrhythmia severity. N = 22 mice for 3 mg/kg dose. N = 35 mice for 30 mg/kg dose. **E.** Total VEB burden in *Casq2*^{-/-} mice treated with vehicle (Veh.) and one week later with *ent*-Vert. N = 57 mice (left panel). Comparison of VEB burden for each mouse before and after all doses and time points for *ent*-Vert treatment (middle panel). Comparison of VT duration for each mouse before and after all doses and time points for *ent*-Vert treatment (right panel). Data in D and E analyzed using Wilcoxon matched-pairs signed rank test.

Figure 3. *ent*-Verticilide (*ent*-Vert) plasma concentrations and corresponding arrhythmia suppression at different time points after intraperitoneal administration of two different *ent*-Vert doses. **A, B.** *ent*-Vert plasma concentration time profiles for 3 mg/kg (**A**, N = 3, 4, 4, 4, 4, 3, 2, 3 and 3 mice (30 total) for each time point) or 30 mg/kg *ent*-Vert (**B**, N = 4, 4, 3, 4, 3, 8, 4, 5, 2, and 3 mice (40 total) for each time point). 1 individual value is not observed in panel A (480 minutes) because the plasma concentration was zero. **C, D.** Arrhythmia suppression measured as percent change in ventricular ectopic beats (VEB) for each mouse comparing *ent*-Vert relative to the week prior with vehicle treatment. (**C**, 3 mg/kg *ent*-Vert, N = 21 mice. **D**, 30 mg/kg *ent*-Vert, N = 35 mice).

Figure 4. *ent*-Verticilide (*ent*-Vert) effect on heart rate. **A, B.** Mice treated with *ent*-Vert had reduced baseline (**A**) and peak (**B**) heart rate. Paired t-test in panel A. Wilcoxon matched-pairs signed rank test in panel B. N = 70 mice. **C, D.** Relationship between *ent*-Vert plasma concentration and baseline (**A**) and peak (**B**) heart rate. No significant correlation was found by simple linear regression analysis (solid blue line with 95% confidence bands shown as dashed lines).

Figure 5. Time dependence and hysteresis of *ent*-Verticilide effect on arrhythmia burden. **A.** Mean plasma concentration (black) and mean inhibition of ventricular ectopic beats (VEB, red) over time for 3 mg/kg dose. Arrhythmia burden was quantified by electrocardiogram recordings approximately 3 minutes prior to plasma collection and data points are offset accordingly. N = 2, 3, 3, and 2 mice for each point, respectively. **B.** 30 mg/kg dose. N = 3, 3, 4, and 3 mice for each point, respectively. **C.** Hysteresis loops for 3 mg/kg dose and **D.** 30 mg/kg dose. Red arrows indicate direction of time.

Figure 6. *ent*-Verticlide (*ent*-Vert) concentration-effect relationship for all mice. Plasma concentrations between 10 – 1440 min after *ent*-Vert administration were binned at 0 (n = 2 mice), 1 – 45.15 (6), 59.83 – 98.43 (6), 114.28 – 149.91 (5), 151.01 – 192.62 (7), 241.30 – 462.48 (6), 534.66 – 760.67 (5), 839.74 – 979.76 (5), 1093.42 – 1566.50 (5), and 1661.61 – 2825.82 (5). Fitting values using non-linear regression to a Hill-function (red line) yielded a 50% inhibitory concentration (IC₅₀) of 266 ng/mL and maximum inhibitory effect (E_{max}) of 93.5%. Data shown as mean ± standard deviation (abscissa) and median ± median absolute deviation (ordinate). N = 52 mice.

Figure 7. Skeletal muscle force measurements in mice treated with vehicle (DMSO + saline), 30 mg/kg *ent*-verticilide (*ent*-Vert.), or 20 mg/kg dantrolene (Dant.) at 0 (pre-drug), 5, 10, and 15 minutes after intraperitoneal administration. Data for each treatment showing the mean force from 75 measurements per mouse at each time point. N = 6 mice per treatment group. Mean values (horizontal black lines) underlay the individual data with connecting lines. Data analyzed by two-way repeated measures ANOVA: treatment effect p = 2.3E-6; time effect p = 9.5E-10; and treatment x time interaction p = 1.7E-13. Follow-up analysis with repeated measures one-way ANOVA with Tukey's post-hoc test for within-group comparisons (* p < 0.01 vs pre-drug) and one-way ANOVA with Tukey's post-hoc test for between-group comparisons (# p < 0.001 vs vehicle).

Tables

PK Parameter	3 mg/kg	30 mg/kg
k_e (hr^{-1})	0.100	0.109
$T_{1/2}$ (hr)	6.92	6.37
T_{\max} (hr)	0.0833	0.0833
C_{\max} (ng/mL)	1460	14100
AUC_{inf} (hr x ng/mL)	959	11100
V_z/F (mL/kg)	31200	24700
Cl/F (mL/min/kg)	52.2	44.8

Table 1. Non-compartmental pharmacokinetic (PK) parameter estimates from naïve-pooled murine plasma concentration-time data following intraperitoneal administration.

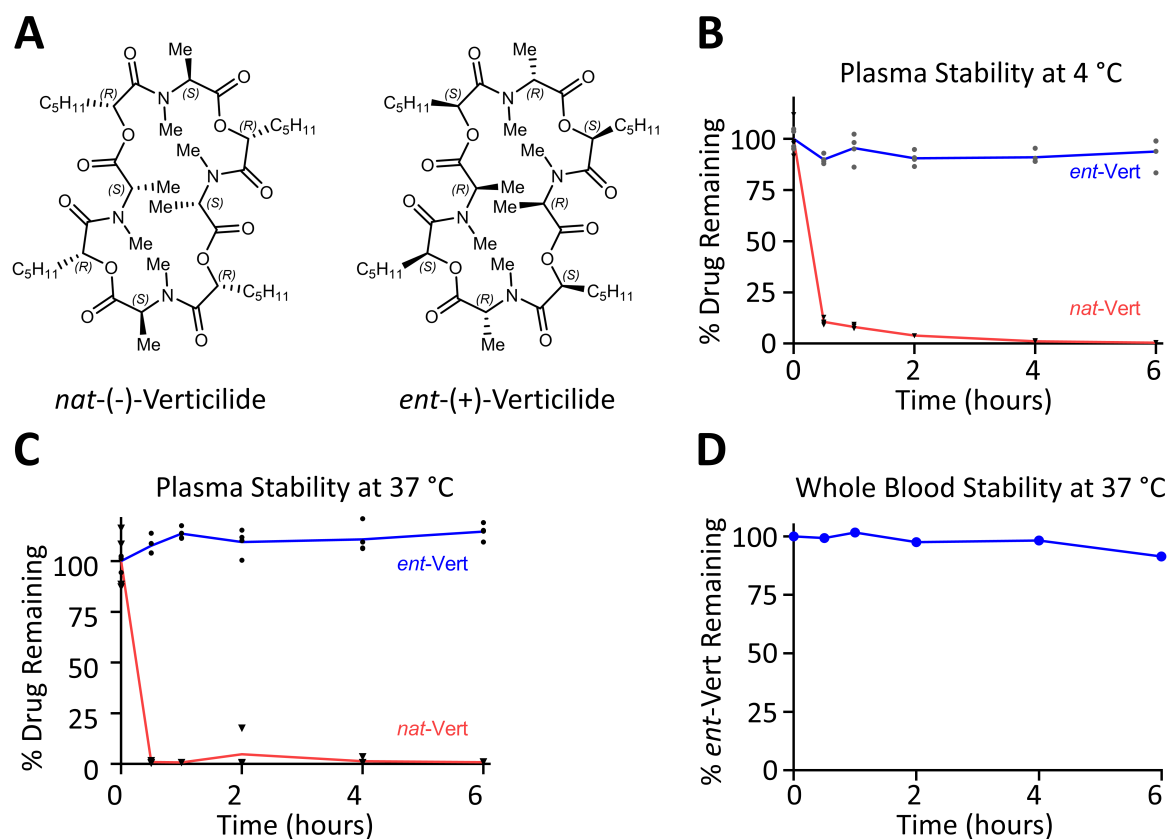


Figure 1

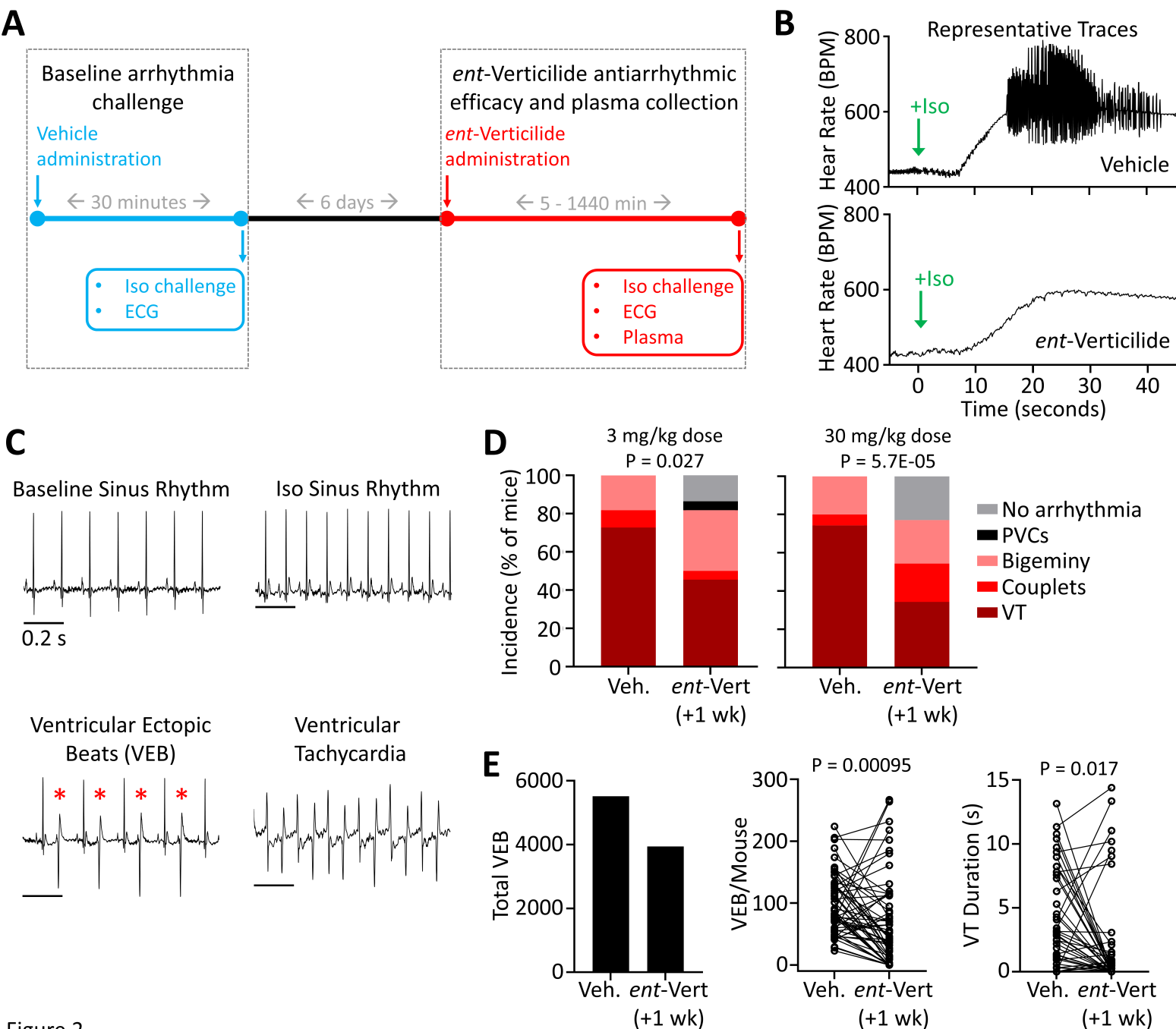


Figure 2

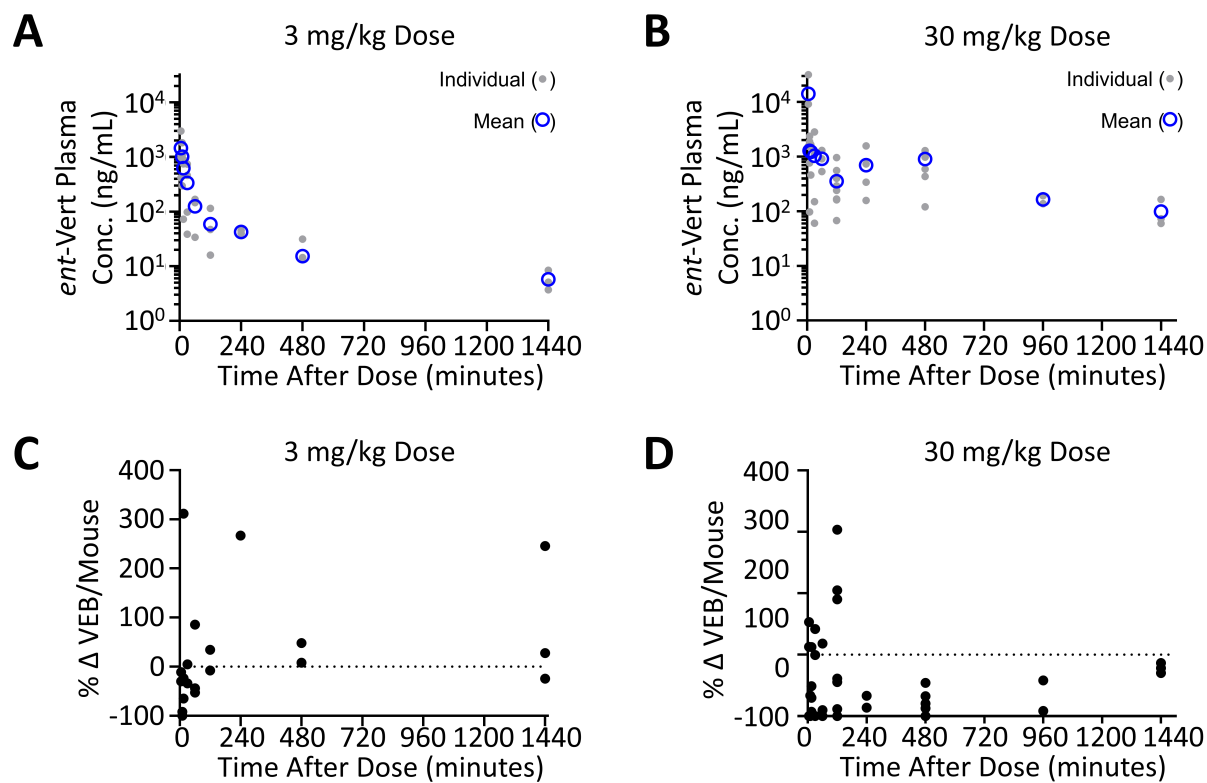


Figure 3

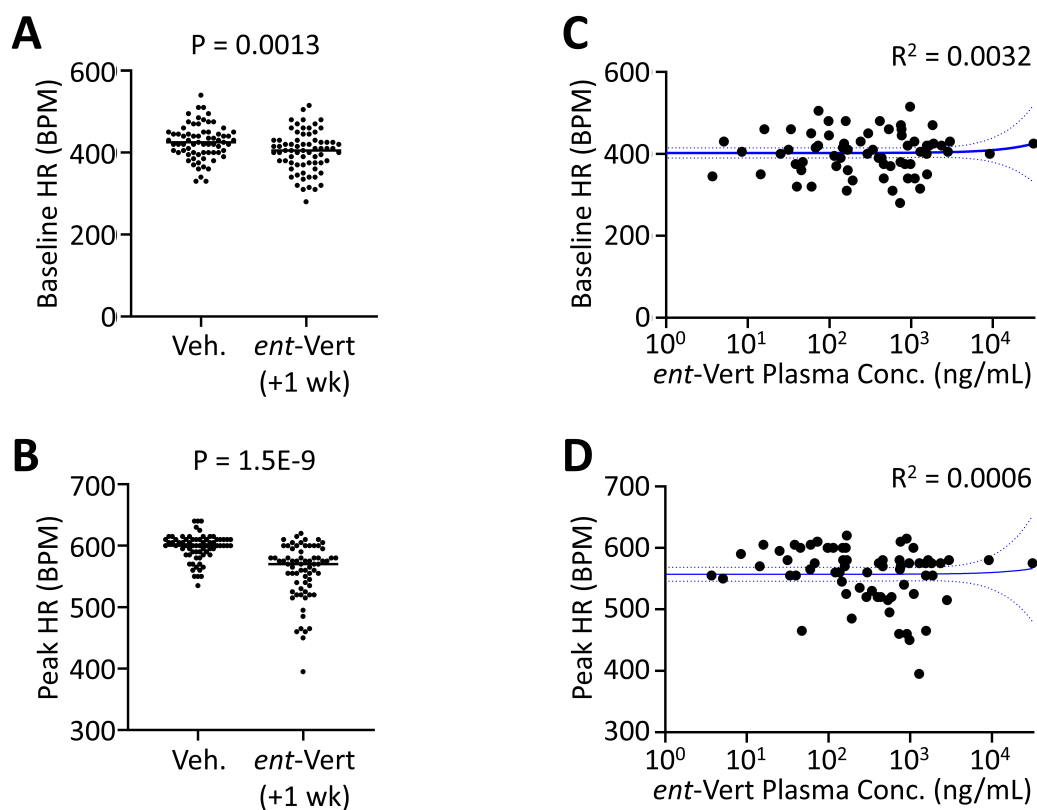


Figure 4

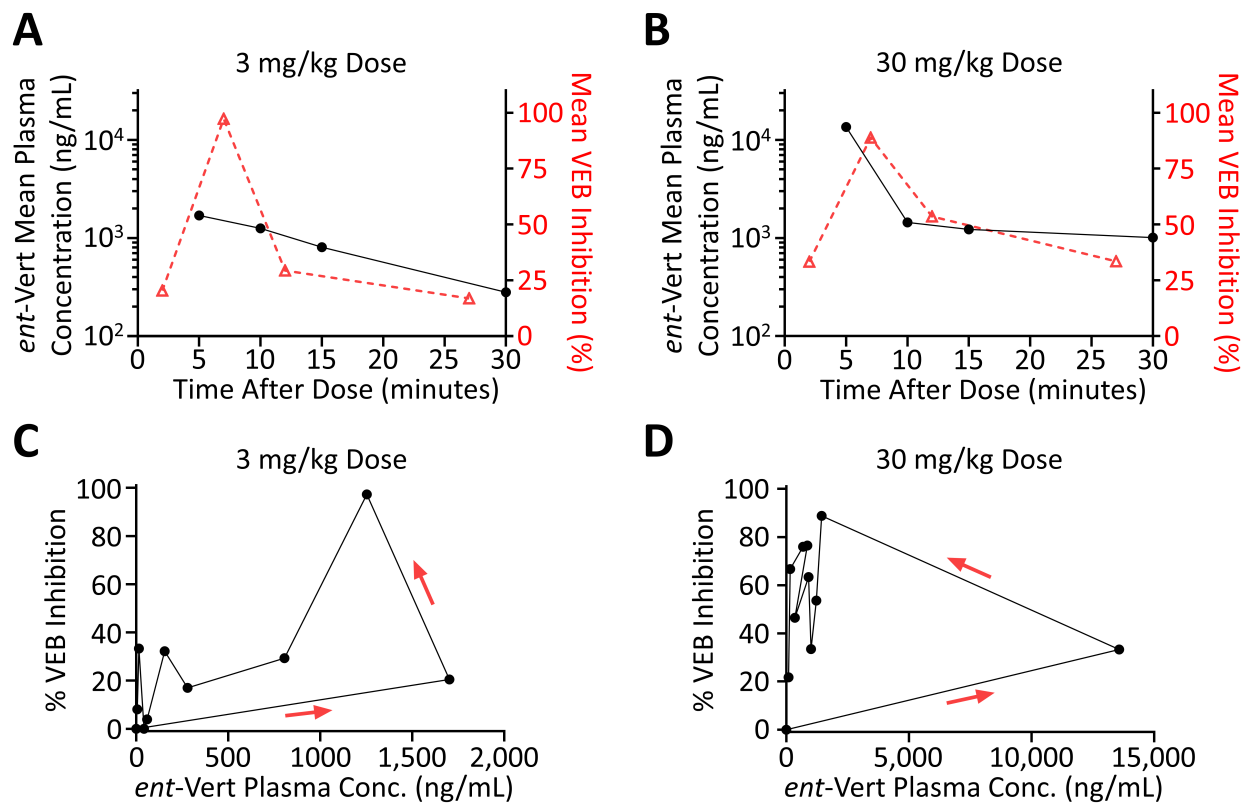


Figure 5

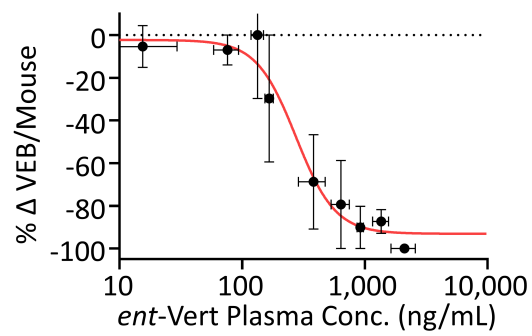


Figure 6

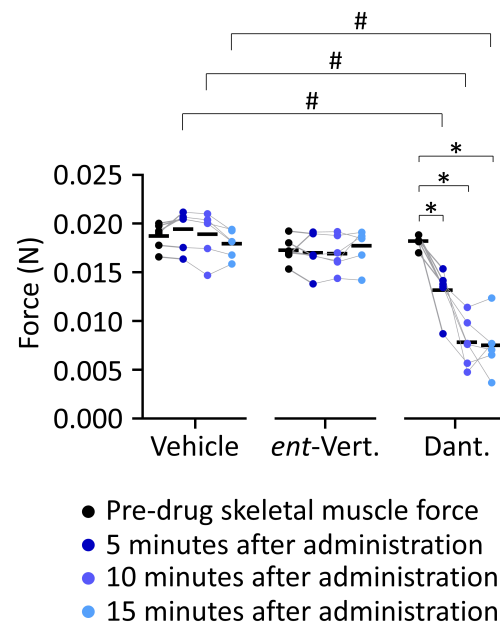


Figure 7